On designing and modelling contraction and sheet wave-energy devices

Onno Bokhove with Grieve, Lee, Naar, Thompson
Seminar at Department of Physics, University of Patras, Greece

School of Mathematics, Leeds Institute for Fluid Dynamics, UK

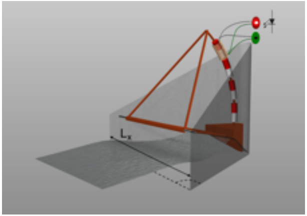

Delft-Toronto-Bristol-Twente-Leeds

- Delft: Molecular dynamics & statistical physics (OB et al. J. Stat. Phys., 1994), incl. Lynden-Bell's work.
- Toronto: Theoretical dynamic meteorology, chaotic Lorenz-1986 system, symplectic integrators.
- Bristol: Shallow-water simulations and magma dynamics (finite-difference hyperbolic systems).
- Twente: Water waves, variational/Hamiltonian dynamics and discontinuous Galerkin FEM.
- Twente/Leeds: Outreach experiments: bore-soliton-splash `https://www.youtube.com/watch?v=YSXsXNX4zW0` to Wetropolis flood demonstrator `https://www.youtube.com/watch?v=yUjYfg2SfY0`.
- Leeds: DA, flood-mitigation cost-effectiveness tool (after 2015 Yorkshire floods), extreme water waves & wave-energy devices.

Tributes to Prof Peregrine† & Prof Kelmanson

Journal of Engineering Mathematics (2026) 157:2
https://doi.org/10.1007/s10665-026-10511-9

Variationally and numerically coupled water-wave and surf zone hydrodynamics

Yang Lu[1] · Floriane Gidel[2] · Tim Bunnik[3] · Onno Bokhove[1] · Mark Kelmanson[1]

Received: 21 August 2025 / Accepted: 13 January 2026 / Published online: 25 February 2026

Abstract
To improve the cost-effectiveness of modelling of wave interactions, a "numerical wavetank" is presented whose distinctive novel feature is its ability to couple both deep-water potential-flow and shallow-water models to controllable, prespecified wavemaker motion and beach topography. The coupling is in part obtained via a variational principle approach that guarantees important conservation properties and numerical stability. The model presented is the first fully nonlinear model to couple deep-water (discretised as finite elements) and shallow-water equations (discretised as finite volumes). Resulting simulations of wave generation, propagation and absorption by shallow-water-wave breaking are presented and analysed. A discussion is given on the efficacy of the novel approach.

Keywords Compatible finite-element method · Finite-volume shallow-water method · Potential-flow water-wave dynamics · Shallow-water surf zone · Variationally coupled dynamics

Variational numerical-modelling strategies for the simulation of driven free-surface waves

Yang Lu[1*†], Floriane Gidel[2†], Junho Choi[3], Onno Bokhove[1*], Mark Kelmanson[1]

[1*]School of Mathematics, Leeds Institute of Fluid Dynamics, University of Leeds, Wood House Lane, Leeds, 100190, United Kingdonm.
[2]SOPHiA GENETICS, Bidart, France.
[3]Mathematical Sciences, Korean Advanced Institute of Science and Technology, Deajeon, South Korea.

*Corresponding author(s). E-mail(s): o.bokhove@leeds.ac.uk;
Contributing authors: floriane.gidel@gmail.com; ;
junho.choi@kaist.ac.kr; markkelmanson@gmail.com;
†These authors contributed equally to this work.

Abstract
A new tool is developed for simulating three-dimensional (3D) water-wave motion using the first fully variational 3D discretisation in space and time of Luke's variational principle (VP), with additional focus on the formation and analysis of extreme waves generated within in-house experimental wavetanks. The resulting "numerical wavetank" is able to emulate laboratory sea states in which complex wave-wave and shoaling interactions occur. After first transforming the time-dependent free surface and oscillatory wavemaker into a static rectilinear domain with fixed boundaries using a σ-coordinate transformation, a fully-variational approach is used to derive a system of weak formulations that leads to a non-autonomous space-discrete Hamiltonian system to which robust (stable and mass-conserving) temporal integrators are applied. Specifically, time-discrete VPs with second-order Störmer-Verlet and modified-midpoint time-integration have been derived (and directly implemented through automation) in the finite-element environment *Firedrake* rather than their explicit weak forms, with spectrally-accurate higher-order finite elements. Verification and validation of the new tool are demonstrated via a novel convergence analysis and comparisons of its numerical results with a new analytical solution of three-dimensional two-soliton interaction as well as data post-processed from wavetank experiments.

Overview of wave-energy research

- Jonathan Bolton provides a worthwhile and excellent overview of wave-energy research in his introductory chapter, including on the contraction device.
- Bolton (2026, PhD thesis, SoM–UoL): "*On the modelling and optimisation of a novel wave-energy device*".

  https://eprints.whiterose.ac.uk/

(i) incoming wave (hydro)dynamics,
(ii) (vertical) buoy motion, and
(iii) power generation.

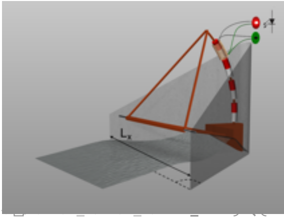

Two devices: contraction buoy & elastomer sheets

M. Jackson, T. Shoyemi & J. Taffs (3rd year ME projects '25/'26).
Buoy in contraction device (3 buoy shapes, 6 frequencies, 8+ resistances):

(a) (b) (c)

Figure 3.1: (a) – Waveflap driven by servo motor (red); (b) – Power supply and control box, green button generates waves, switch allows manual waveflap adjustments; (c) – Buoy, V-channel and induction coils (red) setup.

Two devices: contraction buoy & elastomer sheets

2013 pilot: https://www.youtube.com/watch?v=SZhe_SOxBWo&t=254s

2016 (linear) simulation: https://www.youtube.com/watch?v=ZDsxqPAwP7g

2015 vv. wave tank design:

https://github.com/obokhove/MathslaboratoryUoL/tree/master/wavetank &

https://www.youtube.com/watch?v=3yNoy4H2Z-o (10M views)

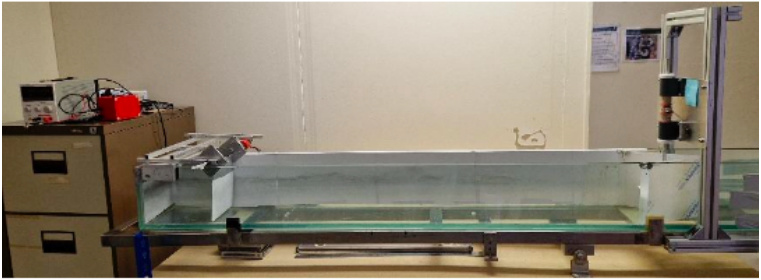

Two devices: contraction buoy & elastomer sheets

3 Elastomer sheets; Eco-Flex Sail, Eco-Flex Surface, PVC Surface:

Figure 5.1 - Schematic of the elastomer energy harvesting experimental setup including sloped beach absorber position.

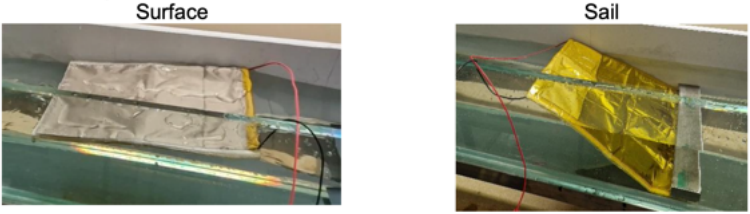

Figure 5.2 - Surface and Sail elastomer geometry configurations used in this chapter.

Different wave amplitudes; plots need power input normalisation (standing/progressive waves):

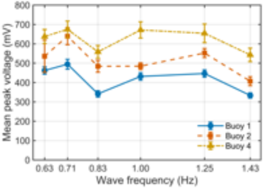

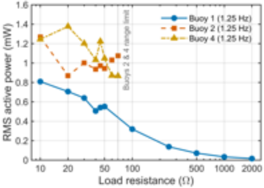

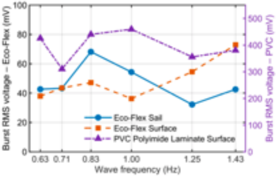

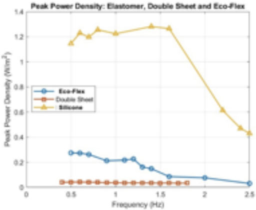

Froude-number scaling

Equate Froude numbers $Fr = \frac{v_{full}}{\sqrt{gL_{full}}} = \frac{v_{scale}}{\sqrt{gL_{scale}}}$ with $s_f = L_{scale}/L_{full} < 1$ (ratio length scales), then:

- Velocity $v_{scale}/v_{full} = \sqrt{L_{scale}/L_{full}} = \sqrt{s_f} < 1.$
- Period or time with $v = L/T$ gives $T_{scale}/T_{full} = \sqrt{s_f} < 1.$
- Force $F = ma$ with $a = v/T$ gives: $F_{scale}/F_{full} = s_f^3 < 1$
- Power $P = Fv$ gives: $P_{scale}/P_{full} = s_f^{3.5} < 1.$

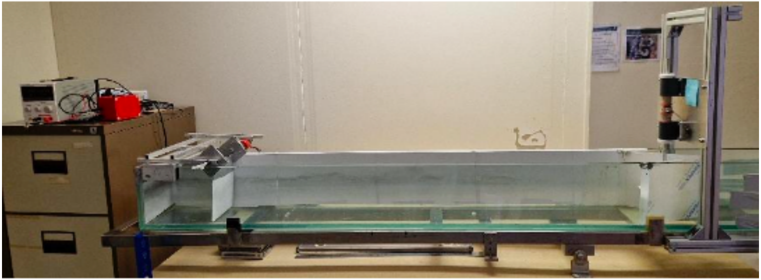

Froude scaling applied: from scale to full model

- Scale model $L_{mod} = 0.2\mathrm{m}$, full device $L_{full} = 8\mathrm{m}$.
- $s_f = 0.025, 1/s_f = 40$.
- Scale buoy power: $1.2\mathrm{mW}$; estimate full buoy power: $\sim 500\mathrm{W}$.
- Yield in passive set-up is very low: shape optimisation & tuned R_{load} like in "*Berkeley wedge*"; or PTO-controller, MOSFET, "negative resistance"?
- Scale PVC power: $\sim 1.3\mathrm{W}/\mathrm{m}^2$ (no load); estimate full PVC sheet power: $\sim 31.5\mathrm{kW}$.
- Cor-Power Ocean buoy $0.3\mathrm{MW}$. Factor 10 off. Optimized impedance-matching circuit needed.

Outline contraction device: modelling components

- Power optimisation of a heaving-buoy wave-energy device considered for a device placed in a wave-amplitude enhancing (V-shaped) contraction.
- Ideally placed in a breakwater or in an array of contractions moored at sea.
- Nonlinear wave-to-wire model consisting of 3 components:

  (i) wave (hydro)dynamics,
  (ii) buoy motion, and
  (iii) power generation.

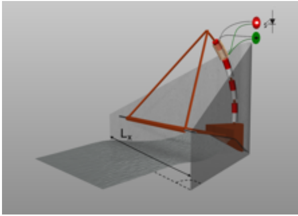

Outline: partitioning & main advances

We have made the following advances for the buoy-generator sub-model (ii-iii):

- Experimental validation of the model hanging from a driven moving point in its dry setting.
- Same length induction coils placed in parallel and rectified generate most power; three-phase rectifier is best.
- NB. Furthered by shown recent advances in ME-projects.

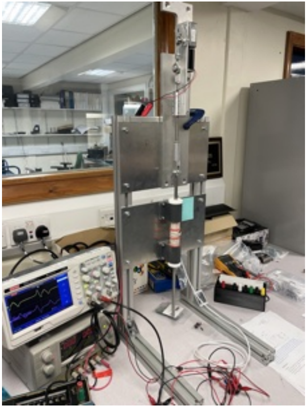

Outline: partitioning & main advances

Advances wave-buoy sub-model (i-ii) are:

- Novel inequality-constraint technique to couple wave and buoy derived and implemented: water surface $\leq$ buoy hull.
- Nonlinear waves: dispersive, depth-integrated (quadratic in z with 2 dofs) Variational Boussinesq or Green-Naghdi Model (e.g. Gagarina et al. 2013).
- Spectrally-accurate 2^{nd}- to 5^{th}-order FEM in 2D horizontal numerical wavetank (open source *Firedrake* environment).

Grand variational principle of wave-to-wire model

Equations of motion follow from variational principle (red=waves, blue=buoy, green=EM-generator, coupling, B. et al. 2019):

$$0 = \rho_0 \delta \int_0^T \int_0^{L_x} \int_{R(t)}^{l_y(x)} \int_0^h -(\partial_t \phi + \frac{1}{2}|\nabla\phi|^2)\mathrm{d}z - gh(\frac{1}{2}h - H_0)$$
$$- \underline{\frac{1}{2\gamma}\Big(F_+(-\gamma(h_b - h) - \lambda)^2 - \lambda^2\Big)}\mathrm{d}y\mathrm{d}x$$
$$MW\dot{Z} - \frac{1}{2}MW^2 - MgZ + (L_i I - \underline{K(Z)})\dot{Q} - \frac{1}{2}L_i I^2 \mathrm{d}t \qquad (1)$$

velocity $\mathrm{u} = \nabla\phi(x,y,z,t)$, depth $h(x,y,t)$, rest depth H_0, e.g. buoy $h_b(Z,y) = Z - K_h - \tan\theta(L_y - y)$, piston $R(t)$, coupling function $\gamma_m G(Z) = K'(Z)$, buoy mass M, keel height K_h, buoy coordinate $Z(t)$, buoy velocity $W(t) = \dot{Z}$, charge $Q(t)$, current $I(t) = \dot{Q}$.

Wave-to-wire: PDEs

- Potential-flow water-wave dynamics (Laplace equation in interior, kinematic & Bernoulli equations at free surface):

$$
\begin{aligned}
\delta\phi : &\quad \nabla^2\phi = 0 \quad \text{in} \quad \Omega\\
(\delta\phi)|_{z=h} : &\quad \partial_t h + \nabla\phi\cdot\nabla h = \phi_z \quad \text{at} \quad z = h\\
\delta h : &\quad \partial_t\phi + \frac{1}{2}|\nabla\phi|^2 + g(z - H_0) - \lambda = 0 \quad \text{at} \quad z = h.
\end{aligned}
$$

- Coupled elliptic Laplace equation to hyperbolic free-surface equations, plus a (Lagrange) **multiplier** λ.

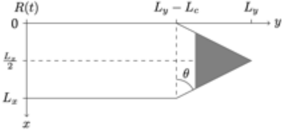

(b) Top view of the tank and buoy, outlining the tank's dimensions and how the buoy fits the shape of the contraction.

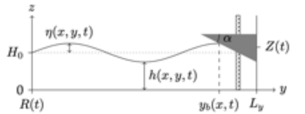

(c) Side view at time t, with the buoy constrained to move vertically.

Wave-to-wire: inequality constraint & ODEs

- Karush-Kuhn-Tucker inequality conditions satisfied at every space-time x, y, t-position are (Burman et al. 2023):

$$\delta\lambda : \lambda = -\max(0, -\gamma(h_b - h) - \lambda) = -\tilde{F}_+(-\gamma(h_b - h) - \lambda)$$
$$\Longrightarrow \underline{h_b(Z, y) - h(x, y, t) \geq 0}, \lambda \leq 0, \lambda(h - h_b) = 0.$$

- Add resistance R_i, R_c & Shockley load $V_s(|I|)$ to submodel:

$$\delta W : \quad \dot{Z} = W,$$
$$\delta Z : \quad M\dot{W} = -Mg \underline{-\gamma_m G(Z) I} - \rho_0 \int_0^{L_x} \int_0^{l_y(x)} \lambda \,\mathrm{d}y\mathrm{d}x$$
$$\delta I : \quad \dot{Q} = I,$$
$$\delta Q ; \quad L_i \dot{I} = \underline{\gamma_m G(Z) \dot{Z}} - (R_i + R_c) I - \frac{I}{|I|} V_S(|I|).$$

Preliminary experimental validation buoy-generator

- Modeled/observed outputs $V(t)$ from one-coil (or 3 coils in series) with 1 bridge rectifier & 3 magnets.
- Simulation of one-coil model with ideal bridge-rectifier: $1/T_{period} = 2.6\mathrm{Hz}$, $R = 100\mathrm{Ohm}$, $l_2 = 0.035\mathrm{m}$. Peak/mean values: $(\underline{1.843}, 0.736)\mathrm{V}$.
- Laboratory observation: $(\underline{1.884}, 0.921)\mathrm{V}$ for $0.8\mathrm{s}$.

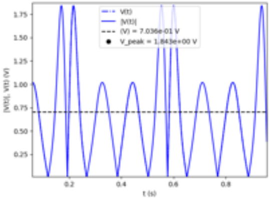

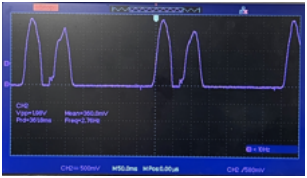

Experimental validation buoy-generator

- Same length coils in series or parallel: 3-phase parallel & rectified best (caveat!):

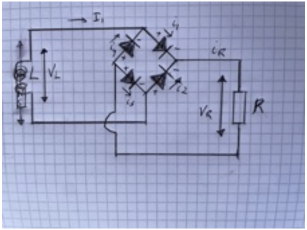

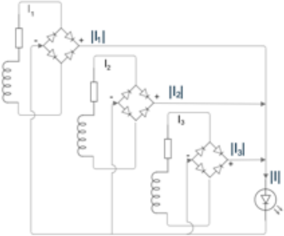

Experimental validation buoy-generator

Table: Measurements for resistances/loads $R = 50, 100, 900\mathrm{Ohm}$.
Set-ups: **S series**: 3 coils in series; 3ph: three-phase rectified of 3 coils; 1ph: 3 coils put in parallel after rectifying each coil; and, only using *Top, Middle or Bottom* coil. (B. et al 2025)

Name 1 magnet	Max, Mean V	Name 3 magnets	Max, Mean V	Comment
1-100-1ph.csv	1.222,0.348	3-100-1ph.csv	2.341,1.122	2nd best
1-100-3ph.csv	1.750,0.725	3-100-3ph.csv	2.500, 1.528	best
1-100-Bot.csv	nan, nan	3-100-Bot.csv	2.155,1.073	glitch
1-100-Mid.csv	1.046,0.337	3-100-Mid.csv	2.346,0.850	2nd best
1-100-S.csv	0.824,0.306	3-100-S.csv	1.884,0.921	
1-100-Top.csv	0.877,0.300	3-100-Top.csv	1.789,0.733	
1-50-1ph.csv	1.107,0.317	3-50-1ph.csv	2.163,1.079	2nd best
1-50-3ph.csv	1.532,0.482	3-50-3ph.csv	2.500,1.435	best
1-50-Bot.csv	0.985,0.258	3-50-Bot.csv	1.896,0.927	
1-50-Mid.csv	0.885,0.299	3-50-Mid.csv	2.045,0.781	
1-50-S.csv	0.635,0.256	3-50-S.csv	1.437,0.703	
1-50-Top.csv	0.767,0.276	3-50-Top.csv	1.584,0.666	

Inequality constraints for BB & device: discretisation

- **Step-1**: Write down the augmented Lagrangian with the inequality constraint embedded and derive the dynamics. *Why?* Includes all dynamics in one VP, in one go.
- **Step-2**: Approximate Lagrange multiplier λ and/or $\tilde{F}_+$ using a new (implicit) superfunction approximation to $\tilde{F}_+(\cdot)$, to solve for λ or $\{\tilde{F}_+, \lambda\}$. *Why?* Dynamics stiff & geometric integrators perform poorly w. (well-)known explicit functions.
- **Step-3**: Write down the new Lagrangian/Hamiltonian dynamics (with λ eliminated). *Why?* Smoothed/simpler.
- **Step-4**: Use Average Vector Field energy (AVF-E) conservation time integrator. *Why?* Only 1 working to date.
- **Step-5**: Test! Derive nonlinear solver stability criterum for Δt. *Why?* Get a handle on time-step size & convergence.

Discretisation strategy: Bouncing Ball –Step-1

- **Step-1**: Define the variations of the augmented Lagrangian $L[Z, W, \lambda]$ for bouncing ball dynamics:

$$0 = \delta \int_0^T L[Z, W, \lambda] \,\mathrm{d}t = \delta \int_0^T W\dot{Z} - \frac{1}{2}W^2 - Z - \frac{1}{2\gamma}\left(F_+(-\gamma Z - \lambda)^2 - \lambda^2\right) \mathrm{d}t.$$

- Definition of variations:

$$\delta \int_0^T L[Z, W, \lambda] \,\mathrm{d}t = \lim_{\epsilon \to 0} \int_0^T \frac{L[Z + \epsilon\delta Z, W + \epsilon\delta W, \lambda + \epsilon\delta\lambda] - L[Z, W, \lambda]}{\epsilon} \,\mathrm{d}t$$

with perturbation functions $(\delta Z)(t) = \delta Z$, $(\delta W)(t) = \delta W$, $(\delta\lambda)(t) = \delta\lambda$ & end-point conditions $\delta Z(0) = \delta Z(T) = 0$.

- Resulting dynamics:

$$\begin{aligned}
\delta W: &\quad \dot{Z} = W\\
\delta Z: &\quad \dot{W} = -1 + \tilde{F}_+(-\gamma Z - \lambda)\\
\delta\lambda: &\quad \lambda = -\tilde{F}_+(-\gamma Z - \lambda) = -F_+(-\gamma Z - \lambda)
\end{aligned}$$

with $\tilde{F}_+(Q) \equiv F_+(Q)F'_+(Q) = F_+(Q) = \max(Q, 0)$.

Discretisation strategy: BB –Step-2

Step-2: In contact dynamics in continuum dynamics, the function $F_+(Q)$ or $\tilde{F}(Q)$ with argument Q often approximated or smoothed, see also ML, by e.g.:

- approximations:

$$\text{Smooth}: \lambda_1(Z) \approx -\, a e^{-\gamma Z/b} = -\tilde{F}_+(Q=-\gamma Z-\lambda),\, Q = b\ln\left(\tilde{F}_+(Q)/a\right) + \tilde{F}_+(Q)$$

$$\text{Asymp.}: \lambda_3(Z) \approx a\min\left(0, \frac{Z}{b} + \frac{Z|Z|}{d}\right), \tilde{F}_+(Q) = \max\left(0, Q + \frac{(d\Gamma - d\sqrt{\Gamma^2 + 4aQ/d})}{2a/\gamma}\right)$$

$$C_2: \lambda_4(Z) \approx a\left\{\frac{Z}{b}, P(Z;\delta), 0\right\} \quad \text{with} \quad P(Z) \in C_2\text{–spline}, \tilde{F}(Q), F(Q) \text{ implicit.}$$

- Geometrically, these are solutions $\lambda = \lambda(Z)$ to $\lambda \leq 0, Z \geq 0, \lambda Z = 0$, i.e. dilineating the fourth quadrant.

Discretisation strategy: BB –Step-3, new Lagrangian

- **Step-3**: Define the variations of the new Lagrangian $L[Z,W]$ for bouncing ball dynamics:

$$0 = \delta \int_0^T L[Z,W,\lambda]\,\mathrm{d}t = \delta \int_0^T W\dot{Z} - \frac{1}{2}W^2 - Z - \int_0^Z \lambda_i(\tilde{Z})\,\mathrm{d}\tilde{Z}\,\mathrm{d}t.$$

- Equations:

$$\delta W: \qquad \dot{Z} = \frac{\partial H}{\partial W} = W$$
$$\delta Z: \qquad \dot{W} = -\frac{\partial H}{\partial Z} = -1 - \lambda_i(Z).$$

- Hamiltonian dynamics for functions $F = F[Z,W]$ with skew-symmetric bracket $\{F,H\}$:

$$\frac{\mathrm{d}F}{\mathrm{d}t} = \{F,H\} = \frac{\partial F}{\partial Z}\frac{\partial H}{\partial W} - \frac{\partial F}{\partial W}\frac{\partial H}{\partial Z},$$

satisfying skew-symmetry $\{F,H\} = -\{H,F\}$ s.t. $\mathrm{d}H/\mathrm{d}t = \{H,H\} = 0$ (and Jacobi's identity).

Discretisation strategy: BB –Step-4, AVF-E

- **Step-4**: AVF energy discrete-time conservation uses the skew-symmetry of the bracket alongside linear expansion $Z(s) = Z^n + s(Z^{n+1} - Z^n), W(s) = W^n + s(W^{n+1} - W^n)$ and $t = s\Delta t, s \in [0, 1]$(e.g. Cotter 2023):

$$
\begin{aligned}
\dot{Z} =& \frac{1}{\Delta t}\frac{\mathrm{d}Z(s)}{\mathrm{d}s} = \frac{Z^{n+1} - Z^n}{\Delta t} = \int_0^1 \frac{\partial H[Z(s), W(s)]}{\partial W(s)}\,\mathrm{d}s\\
&= \int_0^1 W(s)\,\mathrm{d}s = \frac{1}{2}(W^n + W^{n+1})\\
\dot{W} =& \frac{1}{\Delta t}\frac{\mathrm{d}W(s)}{\mathrm{d}s} = \frac{W^{n+1} - W^n}{\Delta t} = \int_0^1 \frac{\partial H[Z(s), W(s)]}{\partial Z(s)}\,\mathrm{d}s = \int_0^1 -1 - \lambda_i\left(Z(s)\right)\,\mathrm{d}s.
\end{aligned}
$$

- For $\lambda_3(Z)$, with $d = b, Z_-^n = \min(0, Z^n)$:

$$
\frac{(W^{n+1} - W^n)}{\Delta t} = -1 - a\Big(\frac{(Z_-^{n+1} + Z_-^n)}{2b} - \frac{((Z_-^{n+1})^2 + Z_-^{n+1}Z_-^n + (Z_-^n)^2)}{3d}\Big)\begin{cases} 1 & Z^{n+1} = Z^n \\ \frac{Z_-^{n+1} - Z_-^n}{Z^{n+1} - Z^n} & \text{else} \end{cases}
$$

Exact integration important to deal with singularity . . . .

Discretisation strategy: BB –Step-4, AVF-E

AVF energy discrete-time conservation uses the skew-symmetry of the bracket alongside linear expansion $Z(s) = Z^n + s(Z^{n+1} - Z^n), W(s) = W^n + s(W^{n+1} - W^n)$ and $t = s\Delta t, s \in [0, 1]$ (e.g. Cotter 2023). Over one time slab, one proves conservation of energy:

$$
\begin{aligned}
H[Z^{n+1}, W^{n+1}] - H[Z^n, W^n] &= \int_0^{\Delta t} \frac{\mathrm{d}H}{\mathrm{d}t}\,\mathrm{d}t = \int_0^1 \frac{\mathrm{d}H[Z(s), W(s)]}{\mathrm{d}s}\,\mathrm{d}s \\
&= \int_0^1 \frac{\partial H}{\partial Z(s)}\frac{\mathrm{d}Z}{\mathrm{d}s} + \frac{\partial H}{\partial W(s)}\frac{\mathrm{d}W}{\mathrm{d}s}\,\mathrm{d}s \\
&= \int_0^1 \frac{\partial H}{\partial Z(s)}(Z^{n+1} - Z^n) + \frac{\partial H}{\partial W(s)}(W^{n+1} - W^n)\,\mathrm{d}s \\
&= \int_0^1 \int_0^1 \frac{\partial H}{\partial Z(s)}\frac{\partial H}{\partial W(\tilde{s})} - \frac{\partial H}{\partial W(s)}\frac{\partial H}{\partial Z(\tilde{s})}\,\mathrm{d}s\,\mathrm{d}\tilde{s} = 0.
\end{aligned}
$$

Discretisation strategy: –BB Step-5

Step-5, using Firedrake FEM framework solvers:

- Parameters $b = 500, \gamma = 1, \Delta t = 0.035$ ($b\gamma = 500, \gamma = 2, 4$ fine too).
- Relationship between b, γ and Δt.
- **PETSc** solvers (to date): *nest, vinewtonrsls*.

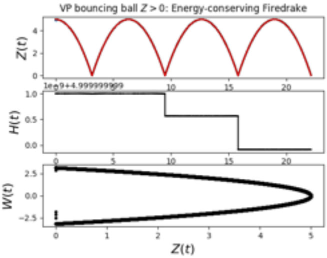

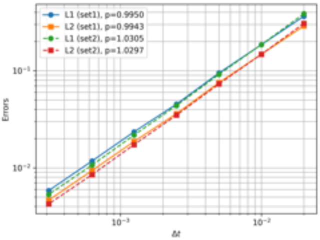

Alternative discretisation –BB

Smooth approximation allows for AVF expression:

$$\tilde{F}_+(Q) = \frac{1}{2}Q + \frac{1}{4}\sqrt{Q^2 + b^2} + \frac{1}{4}\frac{Q^2}{\sqrt{Q^2 + b^2}} \rightarrow_{b\rightarrow 0} \max(0, Q).$$

AVF time discretisation reads:

$$\begin{aligned}
Z^{n+1} =& Z^n + \frac{1}{2}\Delta t(W^n + W^{n+1}),\\
W^{n+1} =& W^n - \Delta t + \frac{1}{4}\Delta t(Q^{n+1} + Q^n)\\
&+ \frac{1}{4}\left(\frac{(Q^{n+1})^2 + Q^{n+1}Q^n + (Q^n)^2 + b^2 + \sqrt{(Q^{n+1})^2 + b^2)}\sqrt{(Q^n)^2 + b^2}}{\sqrt{(Q^{n+1})^2 + b^2)} + \sqrt{(Q^n)^2 + b^2}}\right),\\
0 =& \frac{1}{2}(\lambda^n + \lambda^{n+1}) + \frac{1}{4}\Delta t(Q^{n+1} + Q^n)\\
&+ \frac{1}{4}\left(\frac{(Q^{n+1})^2 + Q^{n+1}Q^n + (Q^n)^2 + b^2 + \sqrt{(Q^{n+1})^2 + b^2)}\sqrt{(Q^n)^2 + b^2}}{\sqrt{(Q^{n+1})^2 + b^2)} + \sqrt{(Q^n)^2 + b^2}}\right)
\end{aligned}$$

with $Q^n = -\gamma Z^n - \lambda^n$ & $Q^{n+1} = -\gamma Z^{n+1} - \lambda^{n+1}$. This is a nonlinear system in $\{Z^{n+1}, W^{n+1}, \lambda^{n+1}\}$.

Alternative discretisation –BB

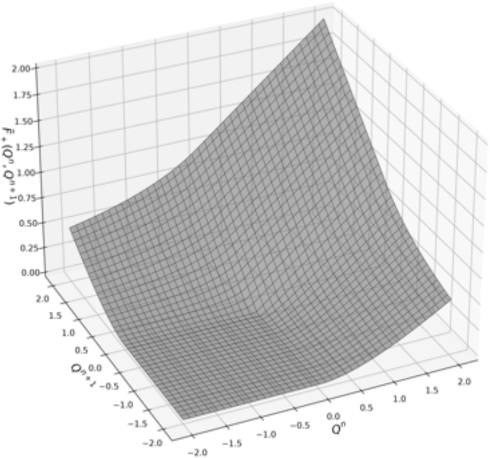

Exact (wire) and smoothed (grey) $\tilde{F}_+(Q^n, Q^{n+1})$–functions, in the AVF time integrator, as used in the algorithms for inequality constraints.

Alternative discretisation –BB

$\sim O(\Delta t)$ when $\gamma = 2.52 \times 10^6\, \Delta t^{-1.99}$, $b = 2.83 \times 10^{-3}\, \Delta t^{0.72}$:

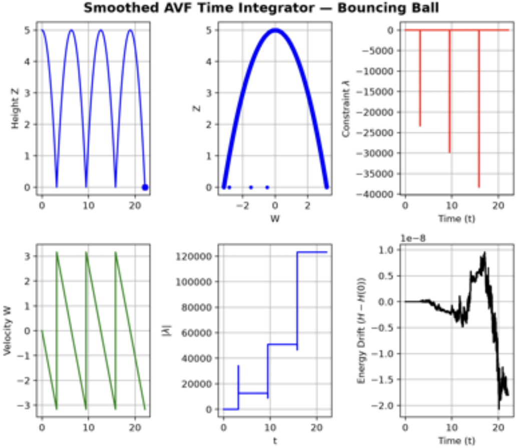

Wave-buoy dynamics: inequality constraints

- Inequality constraints imposed with *derived, smooth* penalty superfunction as Lagrange multiplier (augmented Lagrangian).
- FEM mesh, e.g., with $1^{\mathrm{st}}, 2^{\mathrm{nd}}, 3^{\mathrm{rd}}$ or 4^{th}-order polynomials [dofs: (6,22,50,88)k]; AVF-energy-conservative (-) time integration essential; sofar $\lambda_{1,4}(Z)$ work:

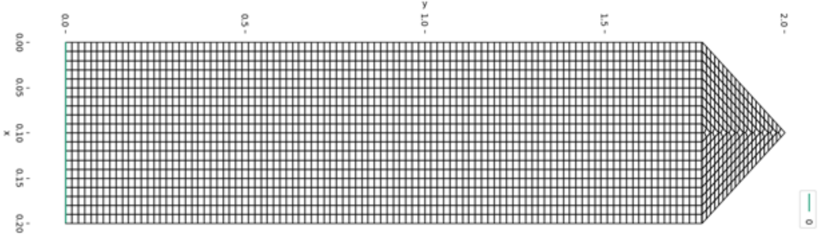

Wave-buoy: full dynamics

- Spectrally accurate Continuous Galerkin (CG) FEM used in space (e.g., 2nd order CG1, CG2, CG3) with time-efficient & error-reducing automatation via & implemented in *Firedrake* environment.
- **Key take-away**: energy conserving 2nd-order AVF discretisation used for stability, in time $t \in [t^n, t^{n+1} = t^n + \Delta t]$.
- Used linear-in-s variables (e.g., Cotter 2023) $\mathrm{q}(s) \equiv \big(Z(s) = (Z^n + s(Z^{n+1} - Z^n), W(s)\big)$ & likewise for $\mathrm{q}(s) \equiv \{h(x,y,s), \phi(x,y,s), \psi(x,y,s), Z(s), W(s), I(s)\}$:

$$\frac{\partial \mathrm{q}}{\partial t} = \frac{1}{\Delta t}\frac{\mathrm{d}\mathrm{q}}{\mathrm{d}s} = J(\mathrm{q}^{n+1/2}) \int_0^1 \frac{\partial H[\mathrm{q}(s)]}{\partial \mathrm{q}(s)}\,\mathrm{d}s,$$

  with **crucial exact integration**.
- Polynomials automated; λ_i's derived/programmed.

Wave-buoy dynamics: initial condition rest state

- Starting point: used continuation for λ_1 in $b = 10, 100, 1000, 2000, 4000$ then nondimensionalisation. λ_4 best to date. Rest system $\{W, \phi\}$ solved, eqns other variables $\{Z, h, \psi, I\}$ enforced to be linear & zero.
- Solvers: "bespoke" for rest state, default for dynamics.

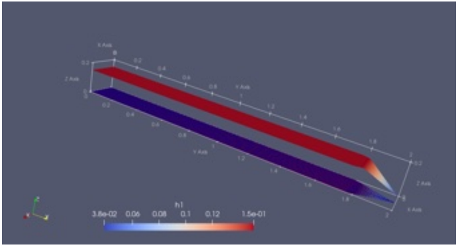

Wave-buoy: full dynamics

- The conservative dynamics has non-canonical components in the variables $\{W, I\}$, which non-constant $J(Z)$-bracket terms, involving the nonlinear function $G(Z)$ arising from solving the 3D Maxwell's equations for axisymmetric induction coil(s), are evaluated at $Z^{n+1/2}$ (per review of Cotter 2023).
- The Variational Boussinesq Model (VBM) is used, a potential flow model with quadratic polynomial accuracy integrated out in z (e.g., Gagarina et al. 2013) with canonical variables $\{h(x, y, t), \phi(x, y, t)\}$ and interior velocity potential degree-of-freedom $\psi(x, y, t)$.

Wave-buoy full dynamics

- Complicated yet polynomial VBM Hamiltonian ($\beta = 1$; Green-Naghdi system when $\beta = 0$), whence AVF-E automation in Firedrake:

$$\begin{aligned}\mathcal{H}[h,\phi,\psi] &= \iint \frac{1}{2}h|\bar{\mathrm{u}}|^2 + \frac{1}{6}h^3\psi^2 + \frac{1}{2}g\left((h+b)^2 - b^2\right) - ghH_0 + \frac{\beta}{90}h^5|\nabla\psi|^2\,\mathrm{d}x\,\mathrm{d}y\\ &= \iint \frac{1}{2}h|\nabla\phi + h\psi\nabla h + \frac{1}{3}h^2\nabla\psi|^2 + \frac{1}{6}h^3\psi^2 + \frac{1}{2}g\left((h+b)^2 - b^2\right)\\ &\quad - ghH_0 + \frac{\beta}{90}h^5|\nabla\psi|^2 + \frac{1}{b^2}e^{-b\left(h_b(Z)-h(x,y,t)\right)}\,\mathrm{d}x\,\mathrm{d}y.\end{aligned}$$

- For simplicity, replaced piston wavemaker by localised body forcing.
- Solvers used default: *CG2* `https://www.youtube.com/watch?v=p7wteD0gMGo`

Wave-buoy dynamics: inequality constraints

- Continuous Galerkin *CG2* [https://youtu.be/bBXuj8XBjAk & https://youtu.be/9ATf-jcHGhs]:

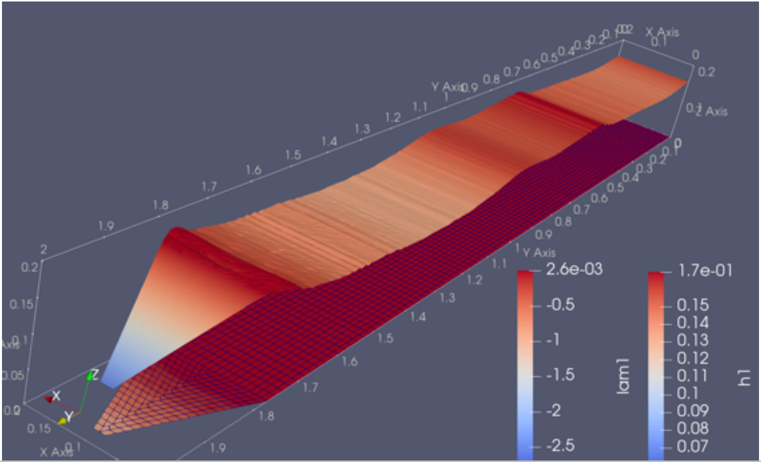

Wave-buoy dynamics: fully coupled single coil, CG2

- For our device, $\lambda_1(h_b - h)$ works poorly since exponential explodes and, hence, $\lambda_4(h_b - h)$ is best $(a = g, b = 10\Delta t^{3/2})$. Crucial C_2 smoothness in $\lambda_{1,4}$ needed. λ_4 still noisy:

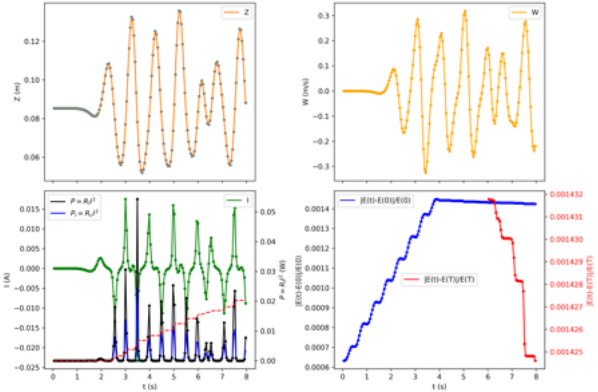

Conclusions

- Buoy-generator lab/simulation models built: 3-phase rectified parallel circuit best by circa $1.5\times$ to $2\times$ (caveats).
- Nonlinear Variational Boussinesq Model coupled to buoy motion via novel inequality-constraint technique: i.e., Firedrake-GitHub [open source `https://www.firedrakeorg.com` –ask]. Thanks to: Colin Cotter!
- Full laboratory validation with nonlinear model underway.
- Optimisation contraction/buoy geometry (e.g. B. et al. IEEE2024), latching & other control.
- **Future**: *elastomer sheet* (manufacturing underway, Jaemin Lee [이 재민], lab and model testing planned using hyperelastic model & VBM).

Thank you very much for your attention ...

- B., Zweers 2013: Proof of principle 2013 https://www.youtube.com/watch?v=SZhe_SOxBWo&t=254s
- B., Kalogirou, Zweers 2019: From bore-soliton-splash to a new wave-to-wire wave-energy model. *Water Waves* **1** 10.1007/s42286-019-00022-9 Bore-soliton-splash: https://www.youtube.com/watch?v=YSXsXNX4zW0&list=FL6mc7mUa6M4Bo2VkD970urw
- B., Henry, Kalogirou, Thomas 2020: *Int. Marine Energy J.*
- Choi, Kalogirou, Lu, B., Kelmanson 2024: A study of extreme water waves using a hierarchy of models based on potential-flow theory. *Water Waves* https://doi.org/10.1007/s42286-024-00084-4
- B., Bolton, Thompson, Geometric power optimisation of a rogue-wave energy device in a (breakwater) contraction. 8^{th} IEEE Conference on Control Technology & Applications (CCTA) (2024) 6 pp. Preprint https://eartharxiv.org/repository/view/7260/
- Lu, Gidel, Choi, B., Kelmanson 2025/26: *Water Waves*. Revision.